Naval Ocean Research and Development Activity
NSTL, Mississippi 39529 NORDA Report 94 April 1985

Airborne Electromagnetic Bathymetry

Final Report

I. J. Won
Kuno Smits
Mapping, Charting, and Geodesy Division
Ocean Science Directorate

Foreword

The Naval Ocean Research and Development Activity has been investigating a possible application of the airborne electromagnetic method to bathymetric charting in a shallow ocean. There is a strong Navy requirement for a rapid, airborne, shallow-ocean bathymetric measurement method that will supplement or even replace the traditional shipborne acoustic sounding methods that are time-consuming and often not suited to shallow coastal areas. Periodical and repetitive bathymetric mapping of heavily trafficked shallow-ocean regions is necessary for meeting specific fleet requirements and for monitoring bottom sediment movements, ship lane maintenance, and a variety of geotechnical operations, as well as for routine charting.

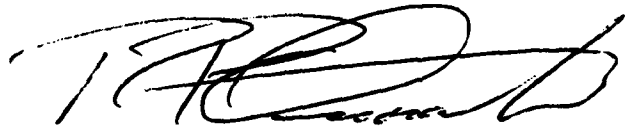

R. P. Onorati, Captain, USN
Commanding Officer, NORDA

Executive summary

An experimental airborne electromagnetic (AEM) survey was carried out in the Cape Cod Bay area to investigate the potential of extracting bathymetric information for a shallow ocean. A commercially available Dighem III AEM system was used for the survey without any significant modification. The helicopter-borne system operated at 385 Hz and 7200 Hz, both in a horizontal coplanar configuration. A concurrent ground truth survey included extensive acoustic soundings, as well as spot water conductivity measurements.

Because of a lack of knowledge about the absolute system calibration figures, an acoustic-sounding calibration was made for each flight line using a small portion of AEM data to derive the zero-level signal, amplitude, and phase calibration factors for each coil pair. The interpreted bathymetric profiles show excellent agreement with corresponding acoustic depth profiles up to one (possibly more) skin depth of the source frequency. It is envisioned that with further improvements in hardware and software, the bathymetric resolution may extend beyond the skin depth. AEM data can also produce (as by-products) conductivity profiles of both seawater and bottom sediments that may find potential applications in mine warfare and offshore geotechnical engineering works.

Acknowledgments

The Airborne electromagnetic feasibility demonstration test and initial data analysis have been funded through PE 63701B by DMA/STT under the program management of CDR Jeff Bodie. The development of improved AEM data interpretation algorithms and final analysis of the demonstration test data have been funded through PE 62759N by ONR Code 220 under the program management of Dr. Tom Warfield. AEM data used in this report were obtained under NORDA Contract Number N62306-84-C-0013. Shallow-water ground truth data were obtained under NORDA Contract Number N62306-84-M-6027 with Woods Hole Oceanographic Institution.

Special appreciation is expressed to the National Oceanic and Atmospheric Administration's ship WHITING for collecting deep-water ground truth data and to Mr. Joseph Heckelman, who was responsible for coordinating NORDA's requirements to NOAA's resources. Appreciation is expressed to Mr. Jim Dodd of the U.S. Geological Survey and the Hydrographic Department under Mr. Robert Higgs at NAVOCEANO for providing Del Norte transponder and Loran-C navigation support. We also thank Dr. Doug Fraser of Dighem, Inc., for many helpful discussions and Dr. Don Durham and Dr. Jerald Caruthers of NORDA for their continued interest and support.

Contents

Airborne electromagnetic bathymetry

Introduction

The Naval Ocean Research and Development Activity (NORDA) has been investigating a possible application of the airborne electromagnetic (AEM) method to bathymetric charting in a shallow ocean. There is a strong Navy requirement for a rapid airborne and cost-effective shallow-ocean bathymetric method capable of supplementing or even replacing the traditional shipborne acoustic sounding methods, which are time-consuming and often not suited to shallow coastal areas. Periodical and repetitive bathymetric mapping of heavily trafficked shallow-ocean regions is necessary for monitoring bottom sediment movements, ship lane maintenance, and a variety of geotechnical operations, as well as for routine charting.

Test survey in Cape Cod Bay

The test survey area and the AEM flight lines are shown in Figure 1. All flights and ground truth surveys were performed during a 3-day period in June 1984. The AEM system used was a commercially available Dighem III, described in detail by Fraser (1978, 1979, and 1981). The system was equipped with two horizontal coplanar coil pairs operating at 385 Hz and 7200 Hz. Both pairs had an 8-m coil separation (an additional coaxial coil pair operating at 900 Hz was deactivated due to an electronic malfunction).

The sensor platform, or bird, towed by a Sikorsky S58T twin-engine helicopter using a 30-m cable, maintained an average altitude range between 40 m and 50 m above the sea surface. The aircraft altitude was measured by a radar altimeter (Sperry Model 220 mounted on the aircraft) that had a manufacturer-specified accuracy of 5%. A total of about 200 line-km AEM data consisting of 13 segment profiles was obtained in three sorties in less than 7 hours. The sampling rate was 1 sec, corresponding to about 50 m along the ground track (about a 3 km/min ground speed). The maximum water depth in the survey area is about 40 m, according to the bathymetric chart (NOAA Chart 13,246).

The flight plan included data collection before and after each profile at an altitude of about 270 m to calibrate the zero-level signal of the receiver coils. In addition, three short calibration flights were made in a location about 15 km east of the Cape, where the bathymetric chart indicated water depth in excess of 60 m. These data were intended to be used for determining the absolute calibration constants for amplitude and phase of each coil pair on an assumption that the water body below may be considered a uniform conductive half-space. It turned out, however, that this calibration method is not accurate enough for the bathymetric processing. As discussed in "Data Calibration," both zero-level signal and amplitude/phase calibration constants are derived from a small portion of each actual flight line data.

Figure 2 shows a raw AEM data profile accompanied by a corresponding radar altimeter profile along Line 5021 (see Fig. 1 for location). Clearly, the AEM data are overwhelmingly correlatable with variations in altitude. A very crude indication of water depth may be observed from the ratio of the quadrature component to the inphase component of the 385-Hz data: the ratio increases with a decreasing water depth. Unfortunately, this relationship is highly nonlinear. Even though the aircraft altitude is maintained mostly within a 10-m range (between 40 m and 50 m), the corresponding variations of the AEM responses amount to more than 500 parts per million (ppm). Owing to the high water conductivity, errors induced by inaccurate altimetry pose a critical problem. At a 45-m bird altitude, a 1% altitude change at a given water depth of 10 m generates amplitude differences of 22 ppm at 385 Hz and 33 ppm at 7200 Hz. It can also be shown that, for a 1-m depth change at the same water depth of 10 m, the predicted amplitude differences amount to only 10 ppm at 385 Hz and 0 ppm at 7200 Hz.

Since the employed radar altimeter has a specified accuracy of 5%, it soon became evident that the radar altitude cannot be trusted for the bathymetric processing. Instead, a new algorithm was developed to use the 7200 Hz response to derive the electromagnetic altitude during the inversion process. The new altitudes thus derived show fairly random zero-biased differences (with respect to the radar altitudes) whose rms amounts to about 2-3%.

Navigation was originally planned to employ a Del Norte navigation system supported by three ground transponders. Excessive distances caused poor reception;

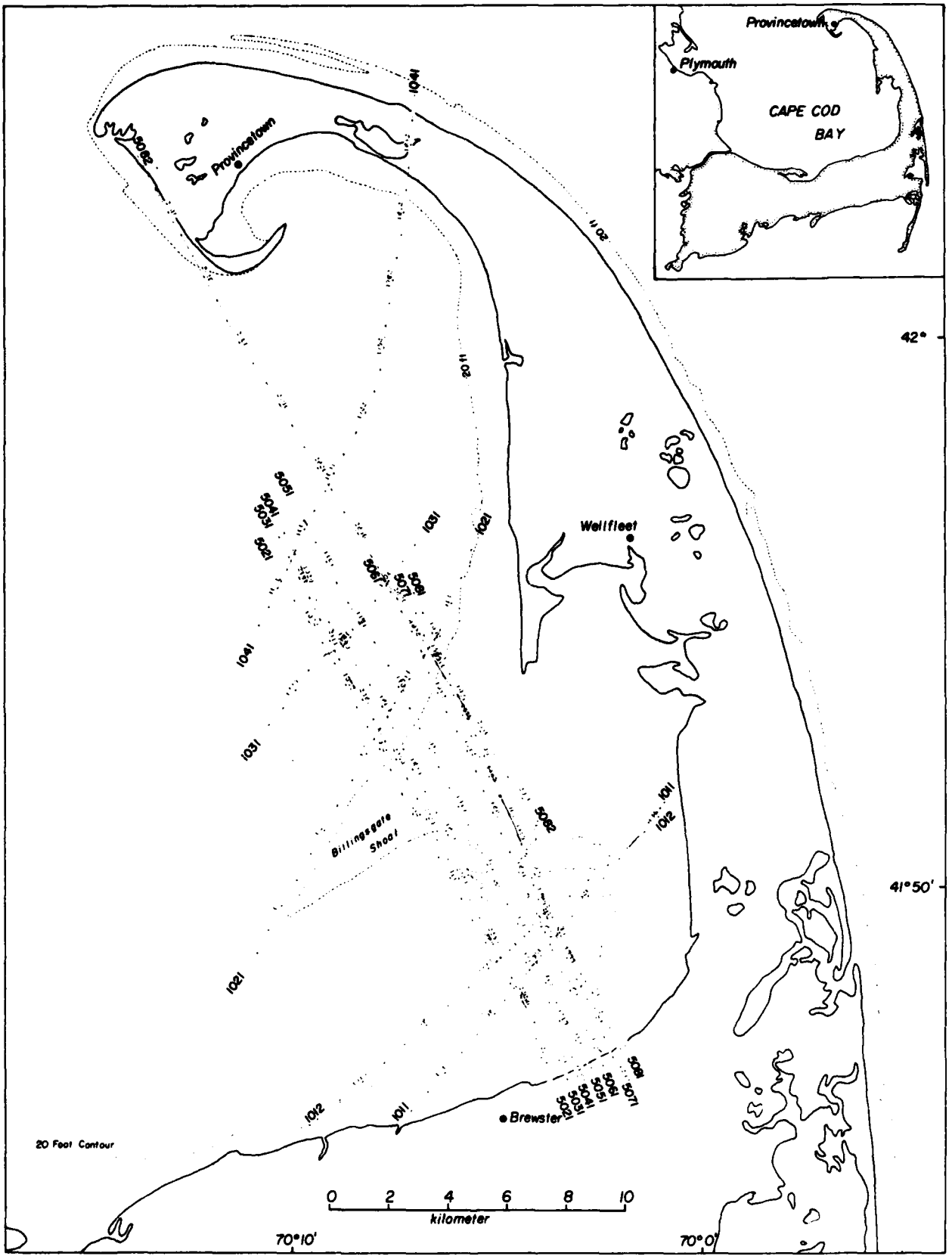

Figure 1. The Cape Cod Bay test area and AEM flight lines. The line numbers are shown on ends of each line. Small numerals are flight fiducials.

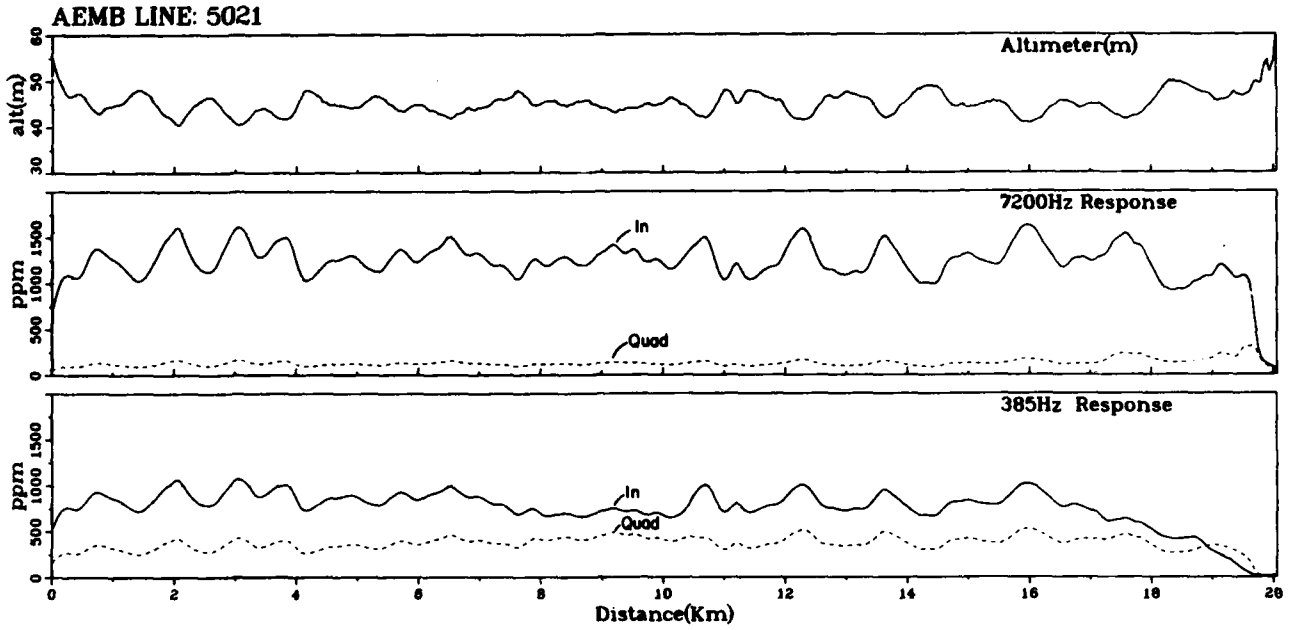

Figure 2. Raw AEM and radar altitude data along Flight Line 5021.

therefore, a Loran-C system was installed on site with a makeshift arrangement of a printer that produced coordinates at a 5-sec interval. These were later interpolated to produce 1-sec interval coordinate data corresponding to the AEM data rate.

A ground truth bathymetric survey concurrent with the AEM flights was carried out using an acoustic depth sounder. A total of about 120 line-km depth profiles was obtained, which covered about 60% of the AEM flight area. Unfortunately, due to many practical reasons, the flight lines and the ship track did not coincide and were often more than 500 m apart. Therefore, the best available ground truth still reflects another interpolated approximation (unless the bottom topography fluctuates rapidly, the ground truth is considered to be accurate within 1 to 2 m).

Spot measurements of water conductivity were made at eight different locations along the ship track at a 3-m depth. They ranged between 4.0 mho/m and 4.12 mho/m. While these values may be fairly representative for deep water, there are considerable uncertainties over very shallow water (< 3 m) where water temperature may rise significantly during the day (particularly during sunny days in June, as in this case). A mere 4°C difference in the water temperature at a given salinity can result in as much as a 10% change in water conductivity. Unfortunately, no ground truth measurements were made during the survey to confirm this possibility.

Interpretation

The high conductivity of seawater (between 3 and 5 mho/m, depending on salinity and temperature with no fresh-water inlets) severely restricts the ability of EM waves to penetrate the water. Bathymetric range and resolution are, therefore, primarily governed by the source frequency. Figure 3 shows the skin depths in a frequency range between 40 Hz and 40 kHz for assumed water conductivities of 2, 3, 4, and 5 mho/m.

For the employed frequencies of 385 Hz and 7200 Hz for seawater with a conductivity of 4 mho/m, we may, therefore, expect skin depth of 12.8 m and 3.0 m, respectively. From Figure 3 the source frequency obviously should be less than 100 Hz to achieve a depth range of 50 m or more.

Fundamental equations for the magnetic field generated by a vertical magnetic dipole located at or above the surface of a layered earth are given by Kozulin (1963) and Frischkneckt (1967). The mutual coupling ratio for a horizontal coplanar configuration, used for the present frequency-domain AEM system, is defined as the ratio of the total magnetic field (H_z) to the primary field (H_z^P):

$$H_z/H_z^P = 1 - a^3 \int_0^\infty \lambda^2 R(\lambda, d, \sigma_1, \sigma_2, h, f) J_o(\lambda a) d\lambda . \quad (1)$$

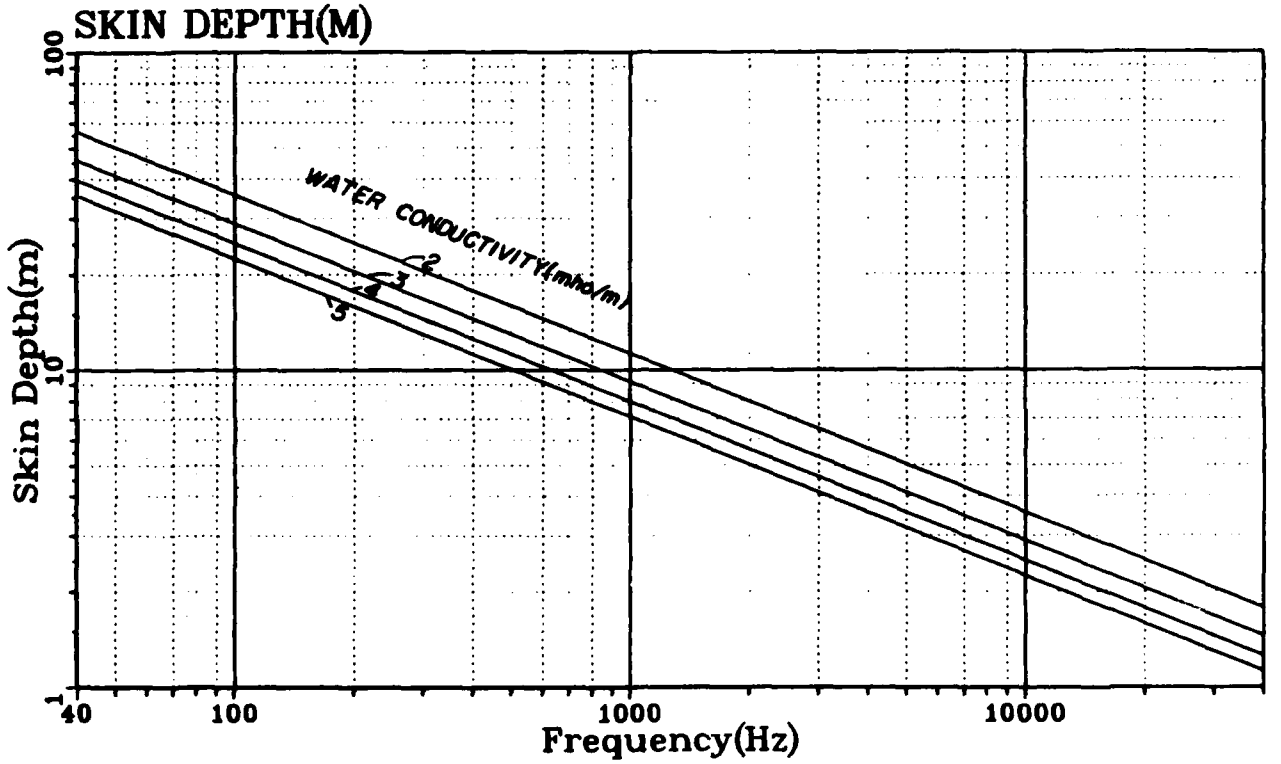

Figure 3. Skin depths as a function of frequency for seawater having a conductivity ranging from 2 mho/m to 5 mho/m.

The kernel function R corresponding to a two-layer earth, of which geometry is shown on Figure 4, can be expressed as

$$R = \frac{V_{0,1} + V_{1,2}\, e^{-2V_1 d}}{1 + V_{0,1}\, V_{1,2}\, e^{-2V_1 d}}, \qquad (2)$$

where $V_{0,1} = (V_0 - V_1) / (V_0 + V_1)$,

$V_{1,2} = (V_1 - V_2) / (V_1 + V_2)$,

$V_0 = \lambda$,

$V_1 = \sqrt{\lambda^2 + i\, 2\pi\, \mu\, \sigma_1\, f}$, and

$V_2 = \sqrt{\lambda^2 + i\, 2\pi\, \mu\, \sigma_2\, f}$.

The mathematical notations in the above expressions are:

- f: transmitter frequency (H_z),
- h: bird altitude,
- a: coil separation,
- d: water depth,
- σ_1: water conductivity,
- σ_2: sediment conductivity,
- μ: magnetic permeability of free space,
- λ: variable of integration, and
- J_o: the zeroth order Bessel function.

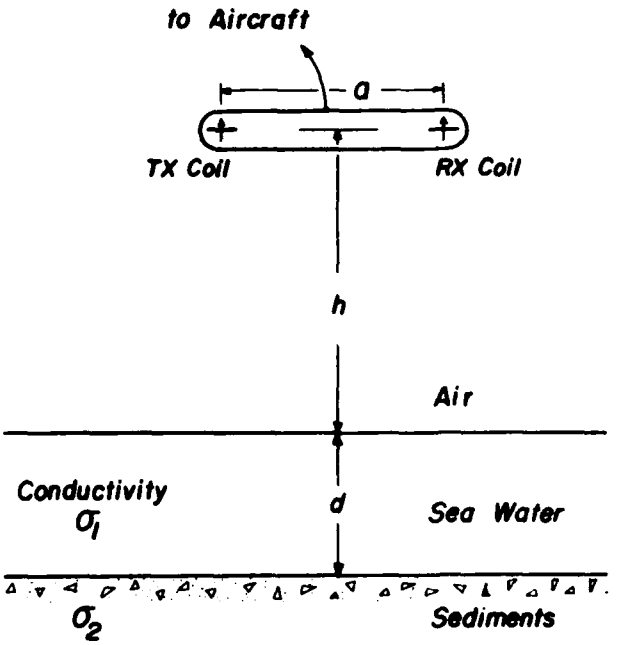

Figure 4. The AEM bathymetric model used for inversion. The unknowns are water depth, conductivities of seawater and bottom sediment, and the bird altitude.

The integral in Equation (1) can be evaluated by the linear digital filter method (Koefoed et al., 1972). We used the filter coefficients published by Anderson (1979b) for the Hankel transform integral.

The first term in Equation (1) representing the primary field is customarily bucked out during measurements, and only the second term representing the ocean response is recorded in a ppm unit. Figure 5 shows computed inphase and quadrature frequency responses in a range of 40 Hz to 40 kHz for various water depths up to 50 m for a 50-m bird altitude, an 8-m coil separation, and conductivities of water and sediment 4 mho/m and 1 mho/m, respectively.

Compared with normal land survey, the ppm responses over an ocean are extremely high due to the highly conductive seawater. It is also noted that the responses are critically sensitive to the bird altitude. The inphase response increases with the source frequency while the quadrature response peaks approximately at a frequency at which the water depth equals the corresponding skin depth. This is previously explained theoretically by Won (1980).

Since we are concerned with the differential changes in the response for varying bathymetric depth, we present Figure 6, which shows the differences of the ppm responses with respect to an infinitely deep ocean having the same 4 mho/m conductivity. We now notice that the total change corresponding to a water depth change from 10 m to 50 m amounts to about 100 ppm. In general, this response increases proportionally to the inverse cube of the bird altitude. It is obvious, therefore, that the recording device must have much larger dynamic ranges than that used for land survey.

Various inversion techniques are presently available to solve for the unknown parameters in Equation (1). These include predominantly several variations of the least-squares method, including the Marquardt algorithm (Marquardt, 1963; Anderson, 1979a) and, occasionally, applications of the generalized inverse theory (Backus and Gilbert, 1967; Fullagar and Oldenburg, 1984; Son, 1985).

The Cape Cod test data were initially interpreted and reported by Fraser (1985) using a least-squares algorithm by Anderson (1979a). Subsequently, the data were reprocessed at NORDA using a different Marquardt least-squares algorithm, notably Subroutine ZXSSQ in the IMSL package. The inverted bathymetry in both cases agreed approximately in trends with known bathymetry but showed a considerable static bias that often exceeded 5-10 m. Further careful inspection of the least-squares inversion results leads us to the following conclusions:

- Computer inversion time is unacceptably long: one-point inversion of the two-frequency data consumes

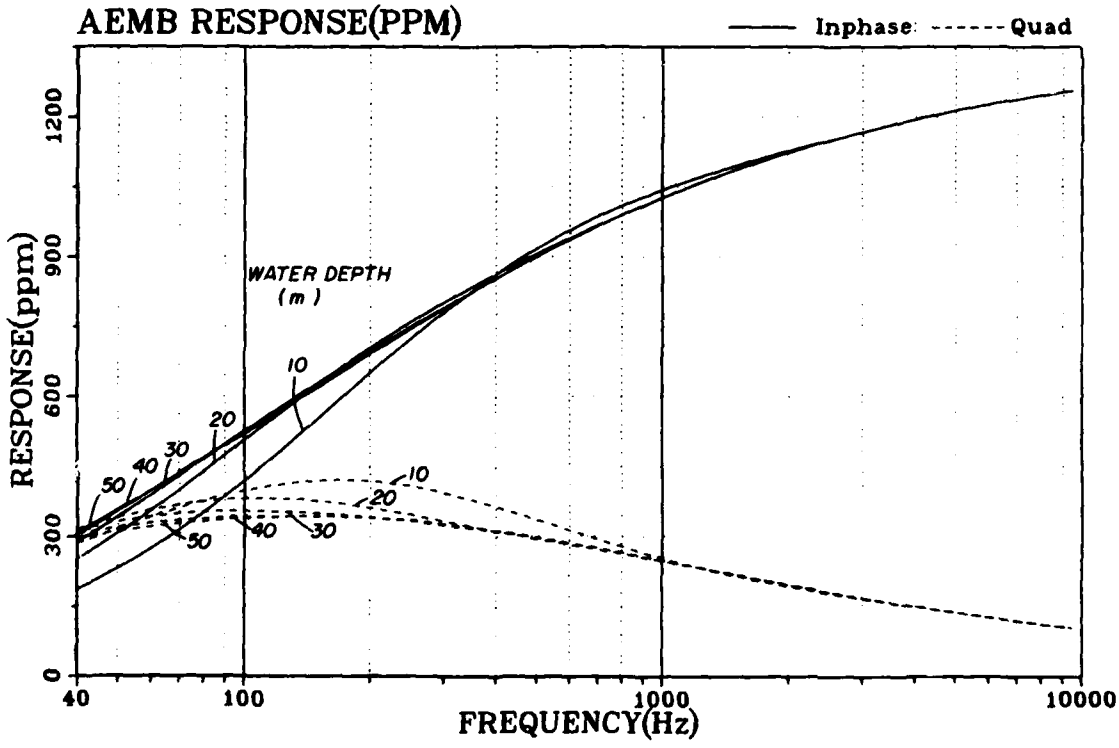

Figure 5. AEM bathymetric responses expressed in ppm for water depths of 10 m, 20 m, 30 m, 40 m and 50 m. The bird altitude is assumed to be 50 m, the coil separation 8 m, water conductivity 4 mho/m, and sediment conductivity 1 mho/m.

from 5 sec to 1 min on a VAX 11/780 computer, even when the water depth is the only sought parameter, while all other parameters are prescribed and fixed.

- AEM response is too sensitive to the bird altitude to accept the specified 5% accuracy of the radar altimeter used for the survey.
- Both the water and the sediment conductivities must be allowed to float albeit in constrained ranges.

The AEM bathymetric profiles reported here are derived from yet another method: analytic solutions of simultaneous nonlinear equations. At each data location, we have four measured quantities; i.e., inphase and quadrature components at two frequencies. From this data set we derive exact solutions of four parameters: water depth, water conductivity, sediment conductivity, and electromagnetic altitude. When unconstrained, the solutions are exact (since the number of knowns and unknowns is the same), resulting in zero residuals regardless of data error. However, severe data error may produce physically unacceptable solutions (e.g., negative depth or conductivities). While least-squares methods (in which the number of knowns is usually much more than that of unknowns) may produce a stable solution set (even though its rms error may be high) from a noisy data set, the present analytic approach is understandably sensitive to data error. Under this circumstance, a low-pass filtering of the inverted profile is justifiable to countermeasure the random data errors.

An inversion algorithm using a modified Newton-Raphson method is then applied to the data. Initially, we derive the sensor altitude and water conductivity from the 7200-Hz data and, subsequently, water depth and bottom conductivity from the 385-Hz data. Inversion time for deriving all four parameters amounts to 0.5 to 2 sec on a VAX 11/780 computer. The analytic method, as in the least-squares method, also requires initial guesses and, to ensure physically acceptable solutions, reasonable solution constraints. The constraints used for the final processing of the Cape Cod data follow.

- Water conductivity (σ_1): 3-5 mho/m
- Sediment conductivity (σ_2): 0.01-2 mho/m
- Water depth (d): 0-50 m
- Altitude (h): positive

Spot measurements of water conductivity at a 3-m depth at eight locations ranged from 4.0 to 4.12 mho/m. No bottom sediment conductivity data are available. However, an extensive in situ study by Hulbert et al. (1982) off the Florida coast shows a common range of 0.4 mho/m to 1.4 mho/m within the first 5-m depth, decreasing only slightly with increasing depth of burial.

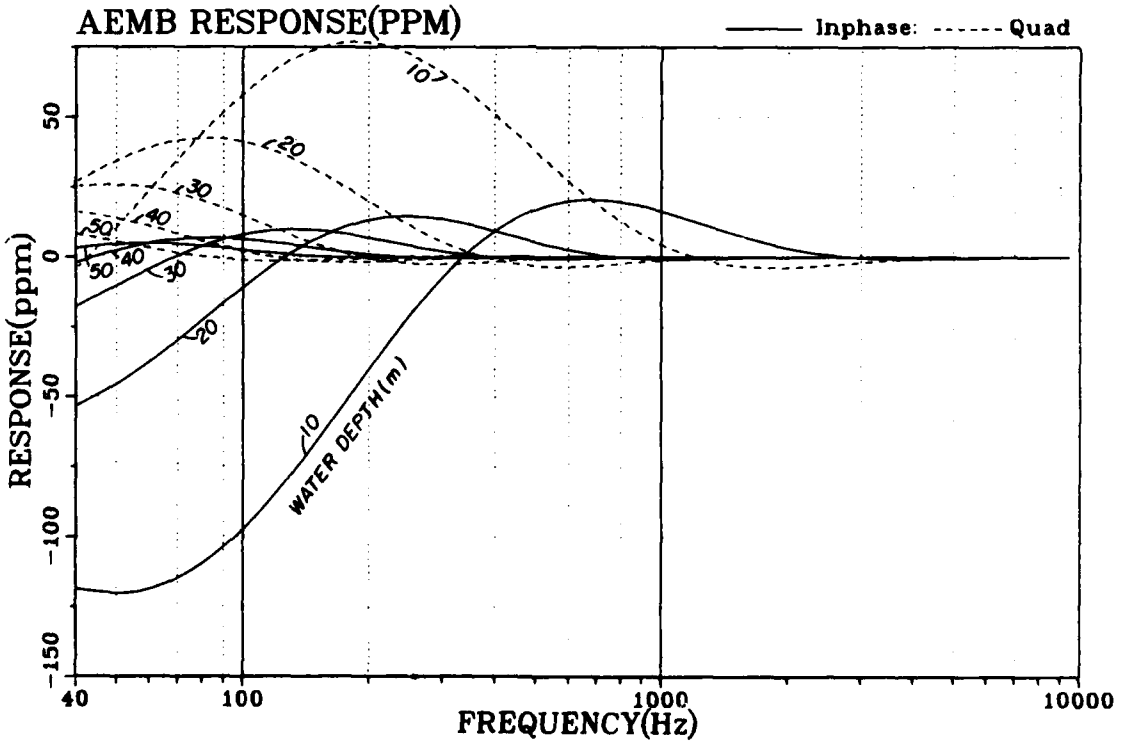

Figure 6. AEM bathymetric response expressed in ppm for water depths 10 m, 20 m, 30 m, 40 m and 50 m relative to an infinitely deep water. The bird altitude is assumed to be 50 m, coil separation 8 m, water conductivity 4 mho/m, and sediment conductivity 1 mho/m.

The inversion process is initiated as follows: For the very first point, we prescribed starting values of σ_1 = 4 mho/m, σ_1 = 1 mho/m, d as read from the hydrographic chart, and h as indicated by the radar altimeter. Once the process starts, the solution set at the present location is prescribed as the initial parameters for the next location. Thus, after the first data point of a profile, the interpretation becomes completely autonomous.

We present only the bathymetric results. Presentation of other parameters will be dealt with in a separate report. It is noted, however, that (1) the derived electromagnetic altitude is well within ±1 m of the radar altitude (less than the manufacturer-specified 5% error), (2) water conductivity is mainly 4 ± 0.2 mho/m except for very shallow-water regions, and (3) bottom sediment conductivity ranges between 0.5 mho/m and 1.5 mho/m in most profiles.

Data calibration

From the beginning it was realized that using an existing commercial frequency-domain AEM system designed for over-the-land survey posed a serious problem in establishing the zero-level signal, and gain and phase calibration factors. Exploration geophysicists usually pay more attention to *relative* anomalies than to their *absolute* values. In the AEM bathymetric survey, we face the challenge of determining the *absolute* values.

An initial attempt to use a set of uniform calibrations (derived from the deep ocean data) for the entire survey data produced unsatisfactory results: while the AEM bathymetry approximately followed known depth profiles, it manifested significant static bias often amounting to 5-10 m.

For the Cape Cod test data, we experimented with three different calibration techniques, viz , zero-level calibration only, amplitude/phase calibration, and zero-level/amplitude/phase calibration. Of these, the last approach turned out to be superior to others in inversion results and was adopted for the final processing.

Calibration factors for selected profiles are listed in Table 1. We note that the amplitude correction factors range between 0 and 7%, the phase correction between 2° and 5°, and the zero-level correction between −28 and −2 ppm. Such insignificant corrections may be quite ignorable for many routine mining exploration problems where only relative anomalies are sought.

The calibration constants are derived as follows: to standardize the process, we choose an arbitrary 50-data point profile segment (about 2.4 km long for the present data) over a relatively flat and deep ocean where an average water depth is known. For each data point, we then prescribe σ_1 = 4 mho/m, σ_2 = 1 mho/m, and h = the radar altitude. The last is the only parameter that varies for each data point. Using these prescribed parameters, we subject the entire segment data set to the Marquardt least-squares inversion to derive the best fit amplitude, phase, and zero-level values. Because of the large data set, the inversion produces very stable calibration factors. These calibration factors are applied to each raw data profile before the final inversion process. It should be pointed out that this known-depth-point calibration method also compensates for the tidal fluctuation, which amounted to a maximum height of 2.8 m during the 7-hour flight period.

Obviously such a hindsight calibration technique is unacceptable: a future production AEM bathymetry system must contain an automatic electronic calibration capability. It should be noted, however, that the data used for the calibration comprise only a fractional segment (about 10%) of a given profile; thus, most of the profile is not directly influenced by the scheme.

Results

Figure 7 shows the interpreted AEM bathymetry for Line 5021 (see Fig. 1 for location). The solid line represents

Table 1. Cape Cod AEM data calibration constants.

Line	385 Hz				7200 Hz			
	Ampl	Phase (deg)	Zero level (ppm) Inphase	Quad	Ampl	Phase (deg)	Zero level (ppm) Inphase	Quad
5021	1.063	2.56	0	−17.1	1.089	2.91	0	−12.7
5031	1.028	3.68	0	− 2.4	1.056	4.30	0	−13.3
5041	1.072	5.20	0	−27.5	1.099	4.90	0	−27.7
5051	1.025	3.49	0	− 5.0	1.054	4.30	0	−17.3
1021	1.040	−0.61	0	38.6	1.078	2.77	0	−14.0
5082	0.996	2.54	0	− 4.3	1.036	2.39	0	− 3.3

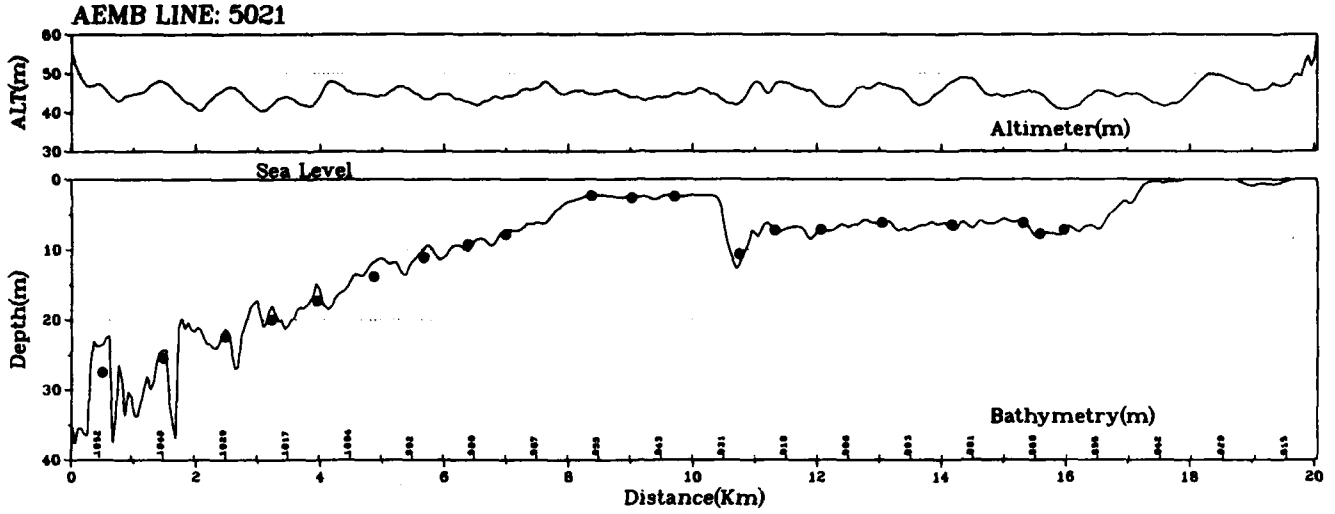

Figure 7. AEM bathymetric profile for Line 5021 along with radar altimeter profile. Solid line represents AEM bathymetry; while solid circles represent depths obtained from a shipborne acoustic profiler. Small numerals at bottom are the flight fiducials.

the water depth inferred from the AEM data. Solid circles denote the depths determined from acoustic profiles. Depths are computed at approximately 50-m intervals. Small numerals at the bottom are the flight line fiducials representing every 20th data point. The profile length is about 20 km.

The agreements are excellent up to a water depth corresponding to about one skin depth (12.8 m) of the 385-Hz signal. In fact, the agreements up to this depth are well within the interpolation accuracy of ground truth data. Below the skin depth we notice progressively degrading resolution resulting in oscillatory bathymetric profiles. Such oscillatory behaviors over deep water

- are common to all AEM bathymetric profiles obtained in the Cape Cod Bay,
- exhibit more or less the same rate of degradation with depth,
- are strongly correlated with variations in the aircraft altitude, and
- appear to be of random Gaussian error (not rigorously determined).

In essence, the oscillatory behavior is a direct result of the decreasing signal-to-noise ratio with respect to the altitude uncertainty. At a 20-m depth, for instance, the maximum theoretical 385-Hz response (against an infinitely deep water) is expected to be about 10 ppm (Fig. 6), while a mere 0.2-m error in altitude will result in the same amount of difference in response. Since the bathymetric errors appear to be random, yet strongly correlated with the aircraft altitude, we tentatively conclude that the error sources are likely related to the altimeter resolution and to such bird attitude uncertainties as pitching and yawing associated with the aircraft altitude variations. The bird attitude can be monitored in the future using inclinometers whose output can be incorporated into the interpretation (Son, 1985).

Such an oscillatory behavior can sometimes be suppressed if we use instead a least-squares inversion method when a sufficient number of redundant measurements is available. The resultant solutions in this case will carry large rms errors, yet may give a deceptively smooth solution profile (errors never die; they simply become hidden in the process). The present analytic inversion method produces zero-residual solutions that fit the observed data regardless of the measurement errors. Although the two approaches are equivalent in the sense of error budgeting, the analytic inversion method appears to be superior in field logistics and in computational speed.

Figure 8 shows the interpretive error profiles for Line 5021. The top figure shows the difference between the radar altitude and the electromagnetic altitude derived from the 7200-Hz record. The differences are mainly less than 1 m, except toward the shoreline where water becomes very shallow and where the interpretative model for the AEM data fails. While the differences appear to be random, they are fairly correlatable with the altitude changes. It is understandable that when aircraft altitude changes, the air speed in general also changes, thus resulting in changes in the towing angle which, in turn, produces a relative motion between the aircraft (on which the altimeter

is mounted) and the bird. This relative motion appears to be responsible for the differences. Mounting the altimeter on the bird may help to resolve this problem in the future.

If we assume that the oscillatory behavior of the AEM bathymetry (Fig. 7) is of random nature, we are justified to perform a low-pass filtering of the interpreted bathymetric profile to render smooth appearances. To this end, we applied to Line 5021 a simple, equal-weight, 11-point running average filter to produce Figure 9. Figures 10-14 show additional AEM bathymetric profiles produced by the above described procedure. The same 11-point filter

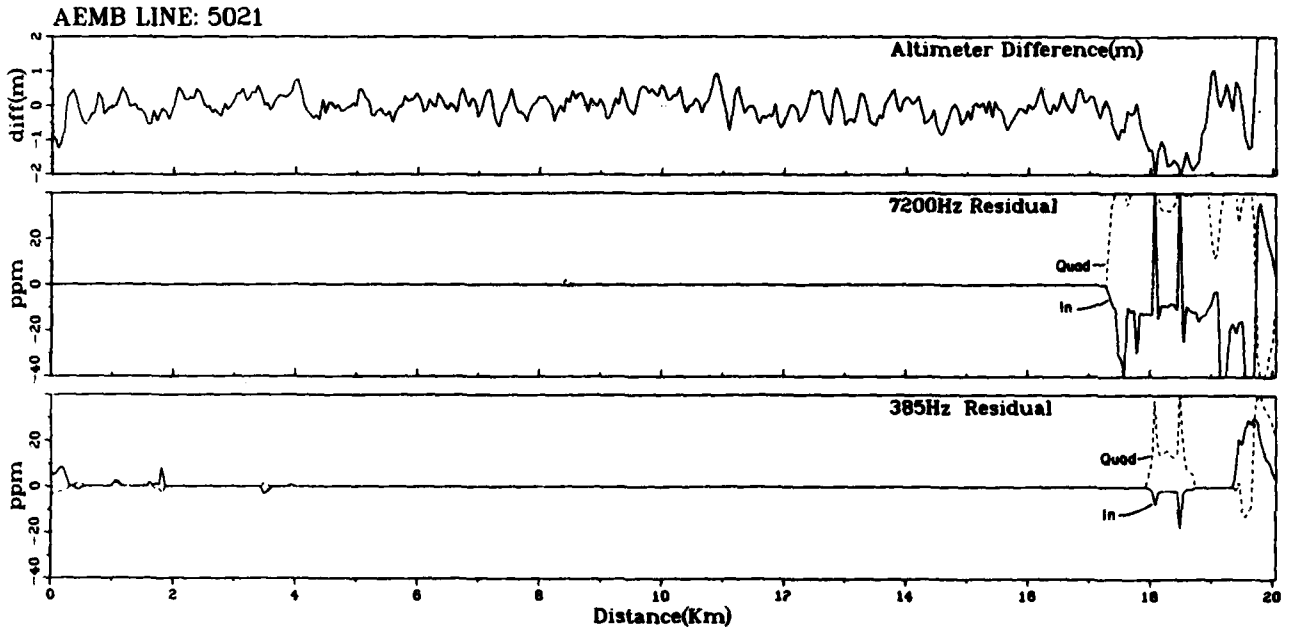

Figure 8. Interpretative error profiles for Line 5021. Top graph shows the differences between the radar altitude and the electromagnetic altitude deduced from the 7200 Hz data. The rest shows differences between measured EM responses and computed EM responses for 385 Hz and 7200 Hz records.

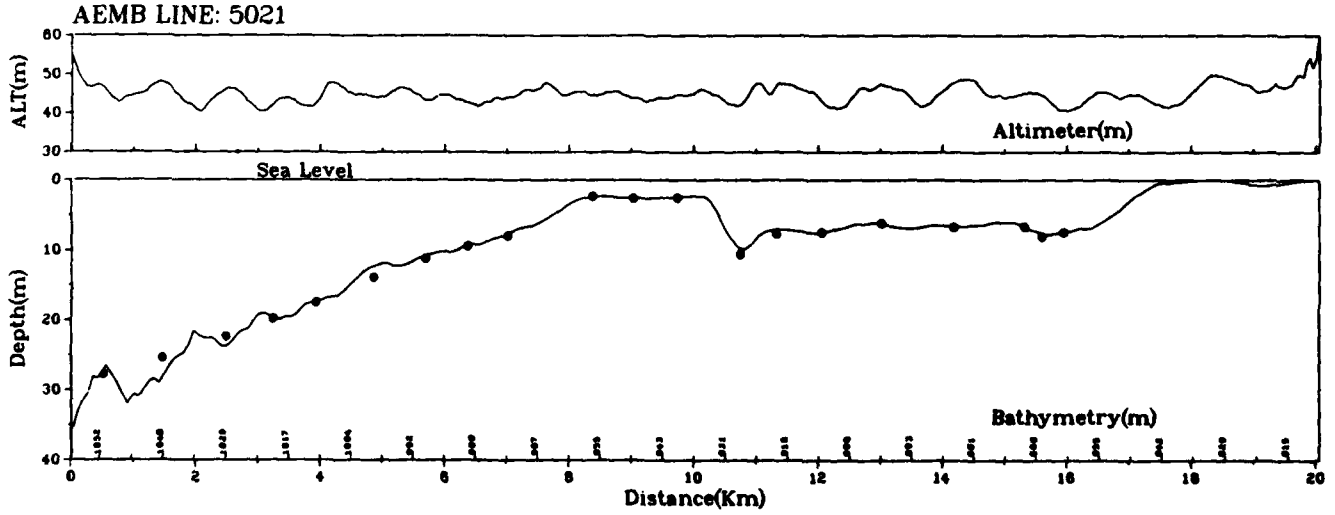

Figure 9. AEM bathymetric profile for Line 5021 after applying an 11-point running average filter. Solid circles represent acoustic depths.

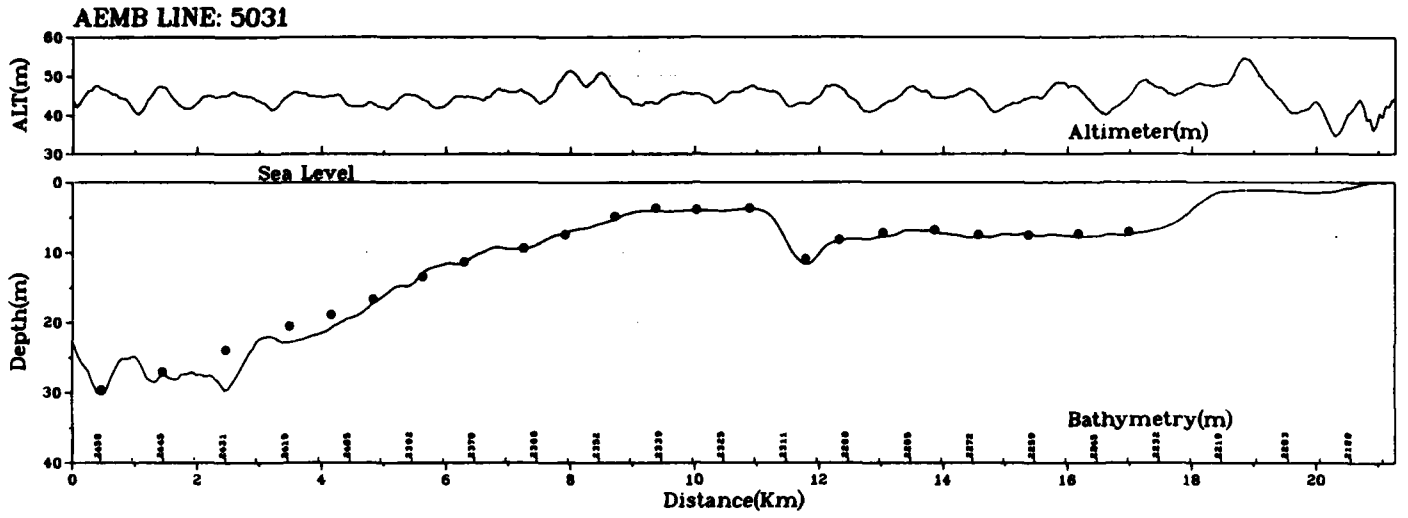

Figure 10. AEM bathymetry profile for Line 5031. Solid circles represent acoustic depths.

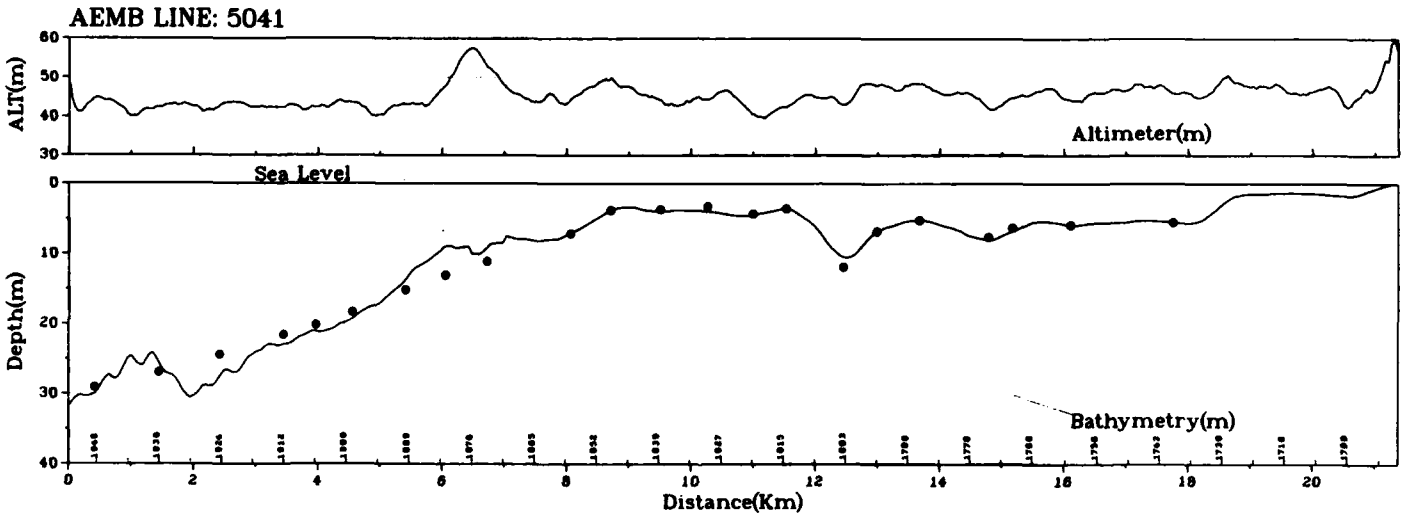

Figure 11. AEM bathymetry profile for Line 5041. Solid circles represent acoustic depths.

has been applied to all profiles. Where the ground truth survey was not performed, we show water depths as read from the bathymetric chart.

A composite of seven AEM profiles is shown in Figure 15. We notice striking details of the sea bottom morphology showing subtle trends and developments of slopes, trenches, and shoals. The fact that each profile is independently derived and yet shows remarkable correlations with neighboring profiles renders further credence to the AEM results.

Conclusions

From our experience through the Cape Cod AEM bathymetry experiment, we summarize some of the error sources that degrade the bathymetric resolution:

- calibration errors: amplitude, phase and zero-level;
- error in the interpretative ocean model, particularly assuming the vertically homogeneous bottom sediment layer;
- altimeter error;

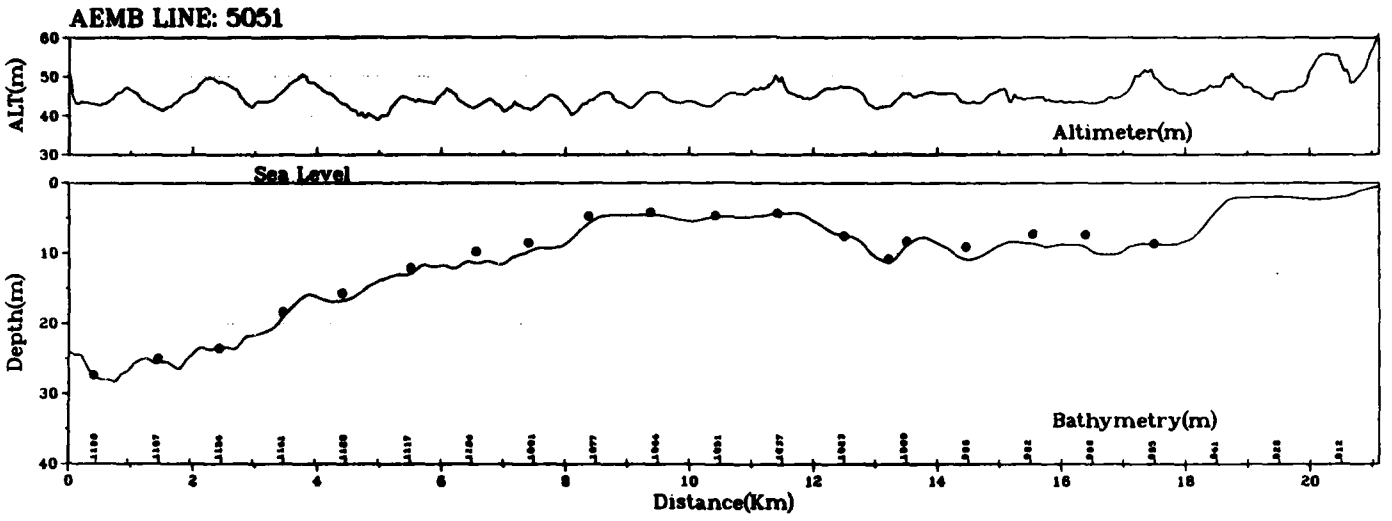

Figure 12. AEM bathymetry profile for Line 5051. Solid circles represent acoustic depths.

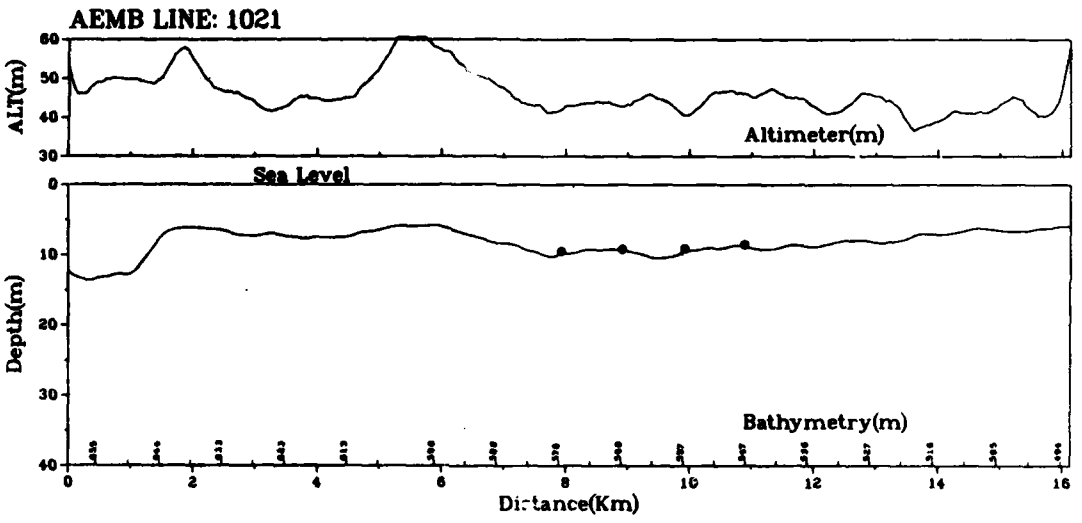

Figure 13. AEM bathymetry profile for Line 1021. Solid circles represent acoustic depths.

- measurement error due to pitching and yawing of the bird—negligible up to 10° if the bird altitude is 50 m or higher;
- ground truth interpolation error due to noncoincidence of tracks by boat and aircraft;
- electronic measurement noise.

Most of the above error sources can be significantly reduced through improvements in equipment and interpretation software.

It is envisioned that with additional research and development efforts, the AEM method will be able to produce accurate bathymetric charts over a shallow ocean (perhaps up to 100 m in depth). Compared with the traditional acoustic sounding techniques, the AEM method can provide an order-of-magnitude faster survey speed at a reduced cost and thus yield a synoptic knowledge of ocean-bottom topography. With improved interpretation schemes, even real-time data processing appears to be a realizable goal.

In addition, the method has potential applications to remote measurements of electrical conductivities of ocean water and bottom sediments. The bottom sediment conductivity, in particular, is closely related to certain

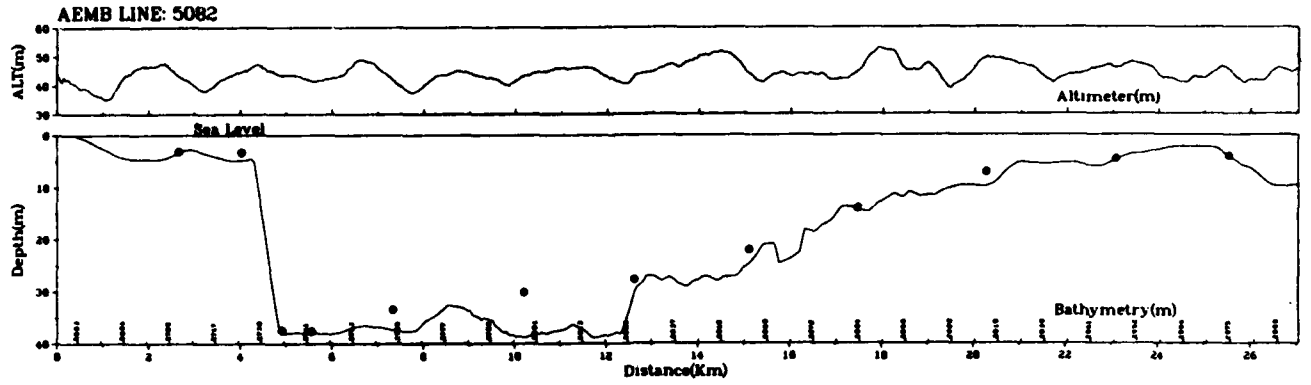

Figure 14. AEM bathymetry profile for Line 5082. Solid circles represent water depths read from the bathymetric chart (NOAA chart: 13,246).

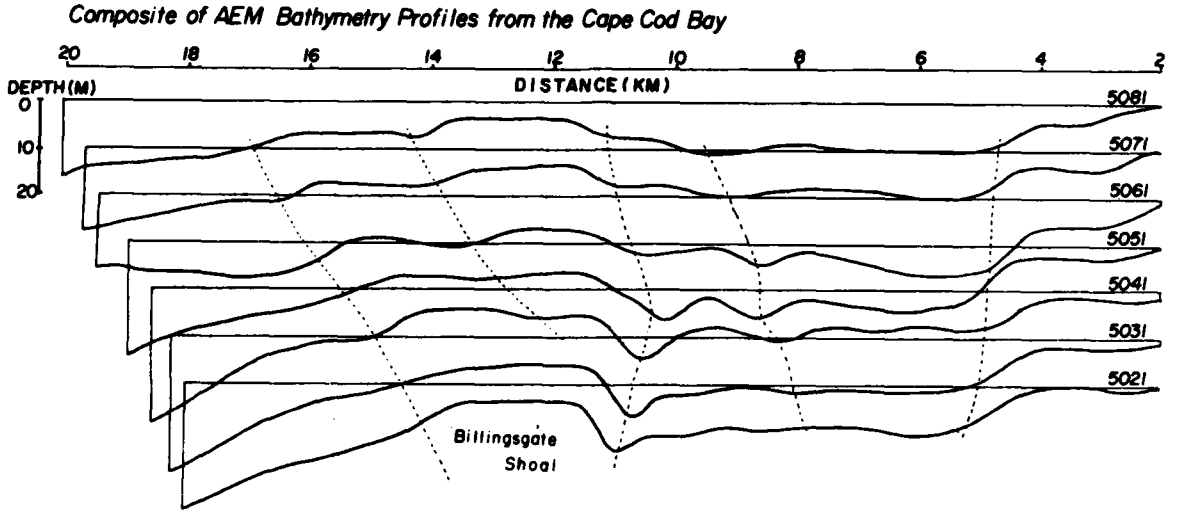

Figure 15. A composite of seven AEM bathymetry profiles from the Cape Cod Bay.

mechanical characteristics, such as compaction rate, porosity, density, and (indirectly perhaps) sediment types, which carry broad geotechnical implications for many offshore activities.

References

Anderson, W. L. (1979a). *Program MARQLOOPS: Marquardt Inversion of Loop-loop Frequency Soundings*. USGS Open File Report 79-240, 75 pp.

Anderson, W. L. (1979b). Numerical Integration of Related Hankel Transforms of Order O and 1 by Adaptive Digital Filtering. *Geophysics*, v. 44, pp. 1245-1265.

Backus, G. E. and F. Gilbert (1967). Numerical Application of a Formalism for Geophysical Inverse Problem. *Geophysical Journal*, Royal Astronomical Society, v. 13, pp. 247-276.

Fraser, D. C. (1978). Resistivity Mapping with an Airborne Multicoil Electromagnetic System. *Geophysics*, v. 43, pp. 144-172.

Fraser, D. C. (1979). The Multicoil II Airborne Electromagnetic System. *Geophysics*, v. 44, pp. 1367-1394.

Fraser, D. C. (1981). Magnetic Mapping with a Multicoil Airborne Electromagnetic System. *Geophysics*, v. 46, pp. 1579-1593.

Fraser, D. C. (1985). *Airborne Electromagnetic (AEM) Bathymetric Survey and Data Analysis, Cape Cod, Massachusetts Area*. Final Report to NORDA, Contract No: N62306-84-C-0013, Submitted by Carson Geoscience Co. Inc., Perkasie, Pennsylvania, 67 pp.

Frischkneckt, F. C. (1967). Field About an Oscillating Magnetic Dipole Over a Two-layer Earth and Application to Ground and Airborne Electromagnetic Surveys. *Quarterly of the Colorado School of Mines*, v. 62, n. 1, pp. 1-370, Golden.

Fullagar, P. K. and D. W. Oldenburg (1984). Inversion of Horizontal Loop Electromagnetic Frequency Soundings. *Geophysics*, v. 49, n. 2, pp. 150-164.

Hulbert, M. H., D. N. Lambert, R. H. Bennett, G. L. Freeland, J. T. Burns, W. B. Sawyer, and P. Field (1982). In situ Electrical Resistivity Measurements of Calcareous Sediments. *American Society for Testing and Materials*, Special Publication STP 777, pp. 414-428.

Koefoed, O., D. P. Ghosh, and G. J. Polman (1972). Computation of Type Curves for Electromagnetic Depth Sounding with a Horizontal Transmitting Coil by Means of a Digital Linear Filter. *Geophysical Prospecting*, v. 20, pp. 406-420.

Kozulin, Y. N. (1963). A Reflection Method for Computing the Electromagnetic Field Above Horizontal Lameller Structures. *Izvestiya*, Academy of Sciences USSR, Geophysics Series (English Edition), no. 3, pp. 267-273.

Marquardt, D. W. (1963). An Algorithm for Least-Squares Estimation of Non-Linear Parameters, *Journal of the Society of Industrial and Applied Mathematics*, v. 11, pp. 431-441.

Son, K. H. (1985). *Interpretation of Electromagnetic Dipole-Dipole Frequency Sounding Data Over a Horizontally Stratified Earth*. Ph.D. thesis, North Carolina State University, Raleigh, 180 pp.

Won, I. J. (1980). A Wideband Electromagnetic Exploration Method—some Theoretical and Experimental Results. *Geophysics*, v. 45, pp. 928-940.

Department of the Navy
Asst Deputy Chief of Naval Materials
for Laboratory Management
Rm 1062 Crystal Plaza Bldg 5
Washington DC 20360

Department of the Navy
Asst Secretary of the Navy
(Research Engineering & System)
Washington DC 20350

Project Manager
ASW Systems Project (PM-4)
Department of the Navy
Washington DC 20360

Department of the Navy
Chief of Naval Material
Washington DC 20360

Department of the Navy
Chief of Naval Operations
ATTN: OP-951, OP 952, OP 954,
OP 980, OP 981D, OP 987, OP-95T
Washington DC 20350

Director
Chief of Naval Research
ONR
ATTN: Code 420 (Dr. G. B. Morris)
Code 425AR (Dr. C. A. Luther)
Code 220 (CAPT Ed Craig)
NSTL MS 39529

Director
Defense Technical Info Cen
Cameron Station
Alexandria VA 22314

Commander
D W Taylor Naval Ship R & D Cen
Bethesda MD 20084

Commanding Officer
Fleet Numerical Ocean Cen
Monterey CA 93940

Commander
Naval Air Development Center
ATTN: Dr. A. R. Ochadlick, Jr.
Warminster PA 18974

Commander
Naval Air Systems Command
Headquarters
ATTN: Code 340J (Mr. Barry Dillon)
Code 330G (Dr. Paul F. Twitchell)
Code 548
Code 330I (Mr. Ted Czuba)
Washington DC 20361

Commanding Officer
Naval Coastal Systems Center
ATTN: Code 4130 (Dr. G. Kekelis)
Code 2110, 3240, 20, 01A
Panama City FL 32407

Commander
Naval Electronic Systems Com
Headquarters
Washington DC 20360

Commanding Officer
Naval Environmental Prediction
Research Facility
Monterey CA 93943

Commander
Naval Facilities Eng Command
Headquarters
200 Stovall Street
Alexandria VA 22332

Commanding Officer
Naval Ocean R & D Activity
ATTN: Codes 100/105/110/111/112
113/115/125L/125P/200/300/350
NSTL MS 39529

Director, Liaison Office
Naval Ocean R & D Activity
800 N. Quincy Street
Ballston Tower #1
Arlington VA 22217

Commander
Naval Ocean Systems Center
San Diego CA 92152

Commanding Officer
Naval Oceanographic Office
ATTN: Codes 8000, 8200, 8400,
8402, and 02
NSTL MS 39522

Commander
Naval Oceanography Command
ATTN: Jerry Reshew
CAPT Neil O'Conner
NSTL MS 39522

Superintendent
Naval Postgraduate School
ATTN: Dr. O. Heinz, Code 61
Monterey CA 93940

Commanding Officer
Naval Research Laboratory
Washington DC 20375

Commander
Naval Sea System Command
Headquarters
ATTN: Daniel Porter, Code 63 R1
PMS-407
Washington DC 20362

Commander
Naval Surface Weapons Center
Dahlgren VA 22448

Commanding Officer
Naval Underwater Systems Center
ATTN: New London Lab
Newport RI 02840

Director
New Zealand Oceano Inst
ATTN: Library
P. O. Box 12-346
WELLINGTON N., NEW ZEALAND

Department of the Navy
Office of Naval Research
ATTN: Code 102
800 N. Quincy St.
Arlington VA 22217

Commanding Officer
ONR Branch Office
536 S Clark Street
Chicago IL 60605

Commanding Officer
ONR Branch Office LONDON
Box 39
FPO New York 09510

Commanding Officer
ONR Western Regional Ofs
1030 E. Green Street
Pasadena CA 91106

Chief of Naval Material
(MAT 0734)
ATTN: Dr. Tom Warfield
800 N. Quincy Street
Arlington VA 22217

Rockwell International
Missile System Division
ATTN: S. Stasenko
3370 Miraloma Avenue
Anaheim CA 92803

NOAA
N/C G2x3
6001 Executive Blvd.
Room 912
ATTN: Mr. Joseph Heckelman
Rockville MD 20852

Norman Albertson
Naval Civil Engineering Laboratory
Port Hueneme CA 93043

CDR Jeff Bodie, USN
Defense Mapping Agency
STT
Bldg 56 Naval Observatory
Washington DC 20305

Ralph Brown
Naval Civil Engineering Laboratory
Port Hueneme CA 93043

CAPT Jon Carlmark, USN
Defense Mapping Agency
Hydrographic/Topographic Center
PRH
Washington DC 20305

Michael Cooper
Naval Coastal Systems Center
Code 4110
Panama City FL 32407

Carlton Duke
Naval Surface Weapons Center
Dahlgren VA 22448

John Brozena
Naval Research Laboratory
4555 Overlook Ave., SW
Washington DC 20375

Howard Carr
Defense Mapping Agency
STT
Bldg 56 Naval Observatory
Washington DC 20305

B. Louis Decker
Defense Mapping Agency
Aerospace Center
2nd and Arsenal Streets
St. Louis MO 63118

George Dupont
Naval Oceanographic Office
NSTL MS 39522

Fred Erskine
Naval Research Laboratory
Code 5160
4555 Overlook Ave., SW
Washington DC 20375

Robert Feden
Naval Research Laboratory
4555 Overlook Ave., SW
Washington DC 20375

Patrick Fell
Defense Mapping Agency
Hydrographic/Topographic Center
STT
Washington DC 20315

CDR Roland Garcia, USN
Naval Oceanography Command
NSTL MS 39529

Jon Hubertz
Coastal Engineering Research Center
P. O. Box 631
Vicksburg MS 39180

David Epp
Office of Naval Research Detachment
NSTL MS 39529

Dennis Franklin
Defense Mapping Agency
STT
Bldg 56 Naval Observatory
Washington DC 20305

Kim Gebhardt
Naval Oceanography Command
NSTL MS 39529

Rolland Hardy
Iowa State University
Ames, Iowa 50011

LT COL Jay Larson, USAF
Defense Mapping Agency
STT
Bldg 56 Naval Observatory
Washington DC 20305

Charles Martin
Defense Mapping Agency
STT
Bldg 56 Naval Observatory
Washington DC 20305

Randall Smith
Defense Mapping Agency
STT
Bldg 56 Naval Observatory
Washington DC 20305

Elroy Soluri
Defense Mapping Agency
Hydrographic/Topographic Center
STT
Washington DC 20315

Mary Lingua
Naval Civil Engineering Laboratory
Monterey CA 93043

George Stanford
Naval Ocean R & D Activity
Code 115
NSTL MS 39529

William Stein
Naval Surface Weapons Center
Dahlgren VA 22448

Edward Thompson
Waterways Experiment Station
Coastal Environment Research Center
P. O. Box 631
Vicksburg, MS 39180

George Walker, Jr.
Naval Oceanographic Office
NSTL MS 39522

Jerome Williams
Oceanography Department
U.S. Naval Academy
Annapolis MD 21402

John Viletto
Engineer Topographic Laboratories
Fort Belvoir VA 22060

Bruce Waxman
Defense Mapping Agency
STT
Bldg 56 Naval Observatory
Washington DC 20305

Department of the Navy
Deputy Chief of Navy Material
for Laboratories
Rm 866 Crystal Plaza 5
Washington DC 20360

Officer in Charge
Naval Underwater Sys Cen Det
New London Laboratory
New London CT 06320

Commander in Chief
U.S. Atlantic Fleet
ATTN: N-37
NRT-2
Norfolk VA 23511

Commandant
U.S. Coast Guard
2100 2nd St., SW
ATTN: C-OSR-2
G-OMI
Washington DC 20590

Commander
Mine Squadron 5
Naval Station
Seattle WA 98115

Commander
Mine Warfare Command
Charleston SC 29408

Commander
Mine Squadron 12
Naval Base
Charleston SC 29408

UNCLASSIFIED

SECURITY CLASSIFICATION OF THIS PAGE

AD-A158640

REPORT DOCUMENTATION PAGE

1a. REPORT SECURITY CLASSIFICATION Unclassified	1b. RESTRICTIVE MARKINGS None
2a. SECURITY CLASSIFICATION AUTHORITY	3. DISTRIBUTION/AVAILABILITY OF REPORT Approved for public release; distribution is unlimited.
2b. DECLASSIFICATION/DOWNGRADING SCHEDULE	
4. PERFORMING ORGANIZATION REPORT NUMBER(S) NORDA Report 94	5. MONITORING ORGANIZATION REPORT NUMBER(S) NORDA Report 94
6. NAME OF PERFORMING ORGANIZATION Naval Ocean Research and Development Activity	7a. NAME OF MONITORING ORGANIZATION Naval Ocean Research and Development Activity
6c. ADDRESS (City, State, and ZIP Code) Ocean Science Directorate NSTL, Mississippi 39529-5004	7b. ADDRESS (City, State, and ZIP Code) Ocean Science Directorate NSTL, Mississippi 39529-5004
8a. NAME OF FUNDING/SPONSORING ORGANIZATION Naval Ocean Research and Development Activity 8b. OFFICE SYMBOL (If applicable)	9. PROCUREMENT INSTRUMENT IDENTIFICATION NUMBER N62306-84-C-0013 N62306-84-M-6027
8c. ADDRESS (City, State, and ZIP Code) Ocean Science Directorate NSTL, Mississippi 39529-5004	10. SOURCE OF FUNDING NOS. PROGRAM ELEMENT NO.: 62759N 63701B; PROJECT NO.; TASK NO.; WORK UNIT NO
11. TITLE (Include Security Classification) Airborne Electromagnetic Bathymetry	
12. PERSONAL AUTHOR(S) I. J. Won and Kuno Smits	
13a. TYPE OF REPORT Final 13b. TIME COVERED From _____ To _____	14. DATE OF REPORT (Yr., Mo., Day) April 1985 15. PAGE COUNT 21
16. SUPPLEMENTARY NOTATION	
17. COSATI CODES FIELD / GROUP / SUB. GR.	18. SUBJECT TERMS (Continue on reverse if necessary and identify by block number) Airborne electromagnetic survey, Cape Cod, bathymetry

19. ABSTRACT (Continue on reverse if necessary and identify by block number)

An experimental airborne electromagnetic survey was carried out in the Cape Cod Bay area to investigate the potential of extracting bathymetric information over a shallow ocean. A commercially available Dighem III AEM system was used for the survey without any significant modification. The helicopter-borne system operated at 385 Hz and 7200 Hz, both in a horizontal coplanar configuration. A concurrent ground truth survey included extensive acoustic profiles, as well as spot water conductivity measurements.

20. DISTRIBUTION/AVAILABILITY OF ABSTRACT UNCLASSIFIED/UNLIMITED ☐ SAME AS RPT. ■ DTIC USERS ☐	21 ABSTRACT SECURITY CLASSIFICATION Unclassified
22a. NAME OF RESPONSIBLE INDIVIDUAL I. J. Won	22b. TELEPHONE NUMBER (Include Area Code) (601) 688-4607 22c. OFFICE SYMBOL Code 352

DD FORM 1473, 83 APR EDITION OF 1 JAN 73 IS OBSOLETE.

UNCLASSIFIED

SECURITY CLASSIFICATION OF THIS PAGE